

**Received:** 2007.04.06  
**Accepted:** 2007.07.24  
**Published:** 2007.10.18

## Monte Carlo study on the impact of spinal fixation rods on dose distribution in photon beams

### Authors' Contribution:

- A** Study Design
- B** Data Collection
- C** Statistical Analysis
- D** Data Interpretation
- E** Manuscript Preparation
- F** Literature Search
- G** Funds Collection

**Asghar Mesbahi**<sup>1,2A,B,C,D,E,F,G</sup>, **Farshad Seyed Nejad**<sup>2A,D,E</sup>

<sup>1</sup> Department of Medical Physics, Medical School, Tabriz University of Medical Sciences, Tabriz, Iran

<sup>2</sup> Department of Radiation Oncology, Imam-Khomeini Hospital, Tabriz, Iran

|                          |   |
|--------------------------|---|
|                          | <h3>Summary</h3>  |
| <b>Background</b>        | <p>Metal spinal rods are used as fixation devices in spinal surgery. The attenuation effect of these rods has not been completely studied for patients with spinal rods and requiring spinal radiotherapy.</p>  |
| <b>Aim</b>               | <p>The purpose of the current study was to investigate the dosimetric perturbation effect of metallic spinal rods in different photon beams.</p>  |
| <b>Materials/Methods</b> | <p>Three photon beams of 6, 9 and 15MV were modelled using MCNP4C Monte Carlo (MC) code. The geometry consisted of two spinal rods at a depth of 4cm and a water phantom was used for MC calculations. The beam profiles at depths of 5.5, 6.5 and 7.5cm were calculated.</p>   |
| <b>Results</b>           | <p>Dose reductions of 10.2–11.2% and 5–6.2% were observed for steel and titanium rods respectively. The insertion of metallic rods into the photon beams did not change the spinal cord received dose but the effect of both types of rods on the target region behind the rods cannot be ignored, especially for steel rods.</p> |
| <b>Conclusions</b>       | <p>Our results suggest that for reliable spinal radiotherapy the dose attenuation effect of spinal rods must be taken into account in treatment planning calculations.</p>  |
| <b>Key words</b>         | <p><b>spinal implants • spinal radiotherapy • Monte Carlo Method • dose attenuation effect</b></p>  |
| <b>Full-text PDF:</b>    | <p><a href="http://www.rpor.eu/pdf.php?MAN=11236">http://www.rpor.eu/pdf.php?MAN=11236</a></p>  |
| <b>Word count:</b>       | <p>1697</p>   |
| <b>Tables:</b>           | <p>1</p>  |
| <b>Figures:</b>          | <p>4</p>  |
| <b>References:</b>       | <p>26</p>   |
| <b>Author's address:</b> | <p>Asghar Mesbahi, Medical Physics Department, Medical School, Tabriz University of Medical Sciences, Tabriz, Iran, e-mail: <a href="mailto:asgharmesbahi@yahoo.com">asgharmesbahi@yahoo.com</a></p>  |

## BACKGROUND

Metal prostheses are used widely in spinal surgery as fixation devices. Spinal rods as part of a spinal stabilization system are applied for fixation purposes [1–3]. There are a small number of patients requiring radiotherapy for plasmacytosis of the lumbar spine or who have other cancers and have spinal prostheses [1,3–6]. The high density and atomic number of these rods for patients undergoing spinal radiation therapy may cause some concerns about the dose inhomogeneities around these prostheses. The mechanical and biological properties of these biomaterials have been studied [1,2,7–9], but their dosimetric effects have not been completely investigated. The most frequently used spinal rods are basically composed of two metallic alloys including titanium and stainless steel. Although there are several published data on the dosimetric effects of hip prostheses [10], only limited research has been performed on the perturbation effect of spinal rods on dose distributions and their implications for treatment planning calculations. To the best of our knowledge there are only three published studies on the dose perturbation effect of spinal implants [4–6]. On the other hand we did not find any document on the dosimetric effects of steel spinal implants in the literature.

A study by Liebross et al. (2002) on the effect of titanium rods on spinal radiotherapy showed underdosage up to 4% and 3% for 6 and 18MV photon beams respectively [4]. This underdosage increased to 13% and 11% for rods with screws for the same photon beams. According to the results of this study, titanium rods did not significantly affect the dose delivered to the spinal cord. Another similar study on titanium rods showed the same results [6]. A recent study on titanium rods on spinal dose revealed a decrease of 5 to 7% for the region behind the rods [5]. Different composition of prosthesis causes different effect on target volume dose. In a study on a hip prosthesis made of cobalt-chromium alloy, a dose reduction of 34% was reported for the target volume in the shadow of the prosthesis [11], but for a titanium hip prosthesis the dose reduction decreased to approximately 10% [12].

Investigations on the impact of a femoral head prosthesis on pelvis radiotherapy have shown that the dosimetric effect of a metal prosthesis cannot be predicted precisely in commercial treatment planning systems [11,13–18]. Monte Carlo (MC) methods have been applied as an alterna-

tive approach for accurate dose calculations in the presence of different tissue inhomogeneities [19–21].

## AIM

In this study the influences of steel and titanium spinal rods on dose distributions were investigated for three photon beams using the MC method.

## MATERIALS AND METHODS

### Monte Carlo modelling and dose calculations

We modelled 6 and 15MV photon beams of a Varian 21EX linac (Varian Medical Systems, Palo Alto, CA, USA) and a 9MV beam of a Neptun 10pc linac (Nuclear Equipment ZdAJ IPJ, Poland) using version 4C of the MCNP radiation transport code [22]. For each photon beam, the head components, including the target, primary collimator, flattening filter, and secondary collimator jaws, were simulated based on manufacturer-provided information. A water phantom with dimensions of 50×50×50cm<sup>3</sup> was simulated under the treatment head to score absolute absorbed dose per incident electron on the target. A mono-energetic electron beam with uniform spatial distribution and 2mm diameter was considered for all photon beams [23–25].

For dose calculations, an initial Monte Carlo simulation of the accelerator head was performed to produce the phase space (PS) file for different energies of the primary electron beam. The PS file was generated by a scoring plane located above the secondary collimators. By running the PS file from the scoring plane the absorbed dose was calculated in the water phantom at a source-to-surface distance (SSD) of 100cm.

For each photon beam, the primary electron beam energy was selected by comparing the measured and calculated percentage depth dose (PDD) curves for 10×10cm<sup>2</sup> field size. After primary electron energy selection, the beam model was commissioned through comparing calculated percentage depth doses and beam profiles with measured data. Then, PDDs and beam profiles for 5×5cm<sup>2</sup>, 10×10cm<sup>2</sup>, and 30×30cm<sup>2</sup> field sizes were calculated and compared with measured data. The beam profiles were calculated at a depth of 10 cm. Photon and electron energy cut-offs of 10 and 500KeV were used for optimum PS file generation. For PDD calculations in the

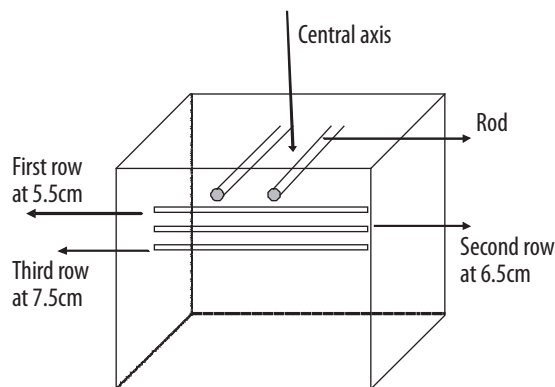


**Figure 1.** Schematic representation of irradiation geometry used for Monte Carlo calculations.

water phantom, a cylinder with radius equal to one-tenth of the beam diameter along the central axis of the beam was considered and divided into scoring cells with a height of 2mm. By running particles in the PS file through the water phantom, the energy deposited in each scoring cell was calculated by \*F8 tally. The same approach was used for the beam profiles, except that the central axis of the scoring cylinder was vertical to the central axis of the beam and the cylinder was at a depth of 10cm. The diameter of the cylinder was 4mm and divided into cells with 2mm thickness along the central axis. Resolution for beam profiles was 2mm laterally. Statistical uncertainty of MC results was less than 1% for PDD and beam profile calculations.

### MC modelling of a spinal rods-like geometry

The geometry used for MC calculations in the presence of spinal rods consisted of a water phantom with dimensions of  $30 \times 30 \times 30 \text{ cm}^3$  and two cylinders resembling the spinal rods with diameters of 6mm and lengths of 20cm located at a depth of 4cm. There was a 4cm gap between two cylinders. Pure steel is not used in implants and usually steel alloys are used. However, based on the information available in the literature and provided by some manufacturers, we used an average density of  $7.8 \text{ g/cm}^3$  with its materials composed of 18% chromium, 12% nickel, and 70% steel for steel rods. For titanium rods, pure titanium was used with density of  $4.5 \text{ g/cm}^3$ . The density and atomic number of rods were entered into the MC input file and considered in the calculations. Three rows of scoring cells at depths of 5.5, 6.5 and 7.5cm were used for beam profile calculations. The dimensions of a dose scoring cell were  $2 \times 2 \times 2 \text{ mm}^3$ . The irradiation geometry is illustrated in Figure 1.

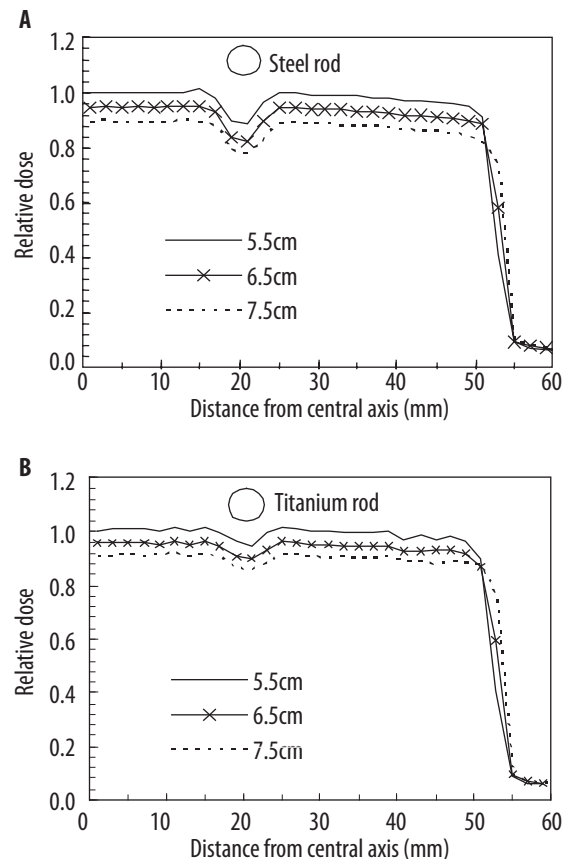


**Figure 2.** The MC calculated beam profiles of a 6MV photon beam with the presence of spinal rods for different depths.

MC calculations were performed for three energies of photons with rods made of steel alloy and pure titanium. Field size of  $10 \times 10 \text{ cm}^2$  with SSD of 100cm was used for calculations.

## RESULTS AND DISCUSSION

### MC modelling validations

Primary electron energies of 6.2, 9.4 and 15.2MeV were selected for 6, 9 and 15MV photon beams respectively. The MC calculated PDD curves and beam profiles were compared with measurements to validate our MC model. There was a good agreement between measurements and calculations for beam profiles and PDD curves. For all photon beams, local differences of less than 2% were seen for PDD values in descending part up to 20cm depth, but it increased up to 18% for the build-up region. For beam profiles, local differences of less than 2% were seen for the flat region, but it increased to 14% for the region located out of field. Our results were consistent with previous study results [23-26] and all the photon beam models were validated in this way.

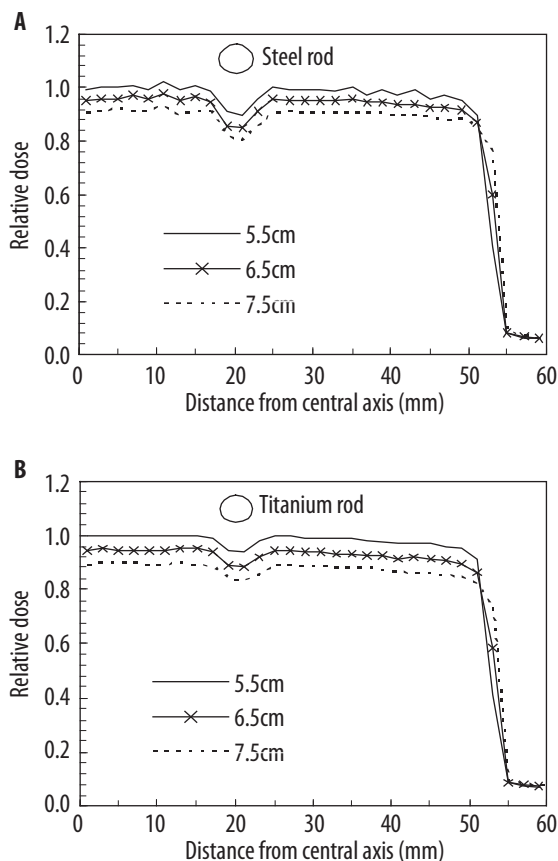


**Figure 3.** The MC calculated beam profiles of a 9MV photon beam with the presence of spinal rods for different depths.

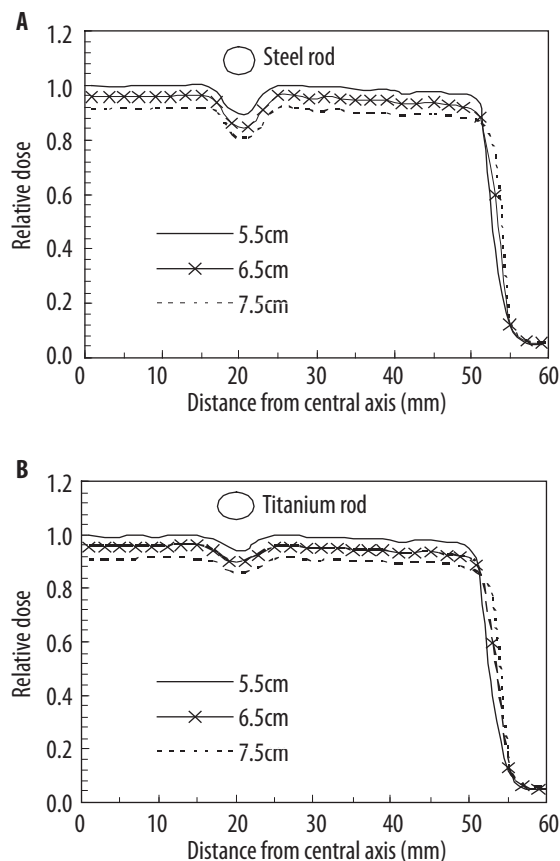


**Figure 4.** The MC calculated beam profiles of a 15MV photon beam with the presence of spinal rods for different depths.

**Table 1.** Dose attenuation of spinal rods made of steel and titanium for different photon beams.

| Depth (cm) | Local dose reduction (%) 6MV |          | Local dose reduction (%) 9MV |          | Local dose reduction (%) 15MV |          |
|------------|------------------------------|----------|------------------------------|----------|-------------------------------|----------|
|            | Steel                        | Titanium | Steel                        | Titanium | Steel                         | Titanium |
| 5.5        | 11.2                         | 5.8      | 11.0                         | 5.6      | 10.5                          | 5.3      |
| 6.5        | 11.2                         | 6.2      | 11.1                         | 5.3      | 10.4                          | 5.2      |
| 7.5        | 10.8                         | 5.87     | 10.6                         | 5.7      | 10.2                          | 5.0      |

**Effect of titanium and steel rods on dose profiles**

The effect of the titanium and steel spinal rods on beam profiles for 6, 9 and 15MV photon beams are shown in Figures 2–4. The profiles of the 6.5 and 7.5cm depths have been normalized to maximum value of the beam profile at the depth of 5.5cm. The maximum attenuation effect of both steel and titanium rods have been calculated and are shown in Table 1.

For both types of rods and all energies, the attenuation effect does not change considerably with depth from 5.5cm to 7.5cm under the rod. It is

seen that the shadowing effect of rods is reduced with photon energy and the maximum range of variation is 11.2–10.4% and 6.2–5.2% for steel and titanium rods at the depth of 6.5cm. The attenuation effect of rods averaged over the depth varies from 11% to 10.4% for steel and from 6% to 5.2% for all photon energies. However, using two parallel opposed or oblique wedged fields may reduce the attenuation effect of spinal rods [4]. The results of the current study are slightly different to the results of the investigation of Weatherburn et al. on titanium rods in which they reported 4% and 3% dose decrease under rods for 6 and 18MV photons respectively. Our attenuation factor is a little higher because of

the higher density of the titanium rods and the depth of dose calculations. They used depths of 5, 10 and 15cm for dose calculations and measurements but the maximum distance of calculation from the rods was 3.5cm in the current study. In a similar study on titanium rods by Lieboss et al, a dose reduction of 6% was seen for the 6MV photon beam, which is in close agreement with our results. In another study by Pekmezci et al., a dose reduction of 5.7% was observed for titanium rods. In our geometry, the received dose of spinal cord was not influenced by spinal rods because the spinal cord was situated in the region between the shadows of spinal rods. In other words, the distance of 4cm between two rods makes it possible for the spinal cord to be prevented from receiving the shadowing effect of implants. However, the target volume behind the spinal rods can be affected and underdosage will happen especially for steel fixation rods in the absence of other compensatory techniques, such as adding other fields.

## CONCLUSIONS

The high density and atomic number of spinal fixation rods attenuate the photon beams approximately 6% to 11% for titanium and steel rods respectively. The shadowing effect of these rods decreases slowly with photon energy. Although it does not change the spinal cord received dose, its dose reduction effect could be significant for the target volume distal to and directly behind steel type stabilization rods. According to previous studies and our results, using multiple fields for treatment of the region behind the rods and accurate calculations of their perturbation effect by treatment planning systems are essential factors in effective radiotherapy of these cases.

## REFERENCES:

1. Aulisa L, di Benedetto A, Vinciguerra A, Lorini G, Tranquilli-Leali P: Corrosion of the Harrington's instrumentation and biological behaviour of the rod-human spine system. *Biomaterials*, 1982; 3: 246-8
2. Dove J: Internal fixation of the lumbar spine. The Hartshill rectangle. *Clin Orthop Relat Res*, 1986; 203: 135-40
3. Hosono N, Yonenobu K, Fuji T et al: Orthopaedic management of spinal metastases. *Clin Orthop Relat Res*, 1995; 312: 148-59
4. Lieboss RH, Starkschall G, Wong PF et al: The effect of titanium stabilization rods on spinal cord radiation dose. *Med Dosim*, 2002; 27: 21-4
5. Pekmezci M, Dirican B, Yapici B et al: Spinal implants and radiation therapy: the effect of various configurations of titanium implant systems in a single-level vertebral metastasis model. *J Bone Joint Surg Am*, 2006; 88: 1093-100
6. Weatherburn H, Safadi N, Saeedi F, Malaker K: Titanium Spinal Prostheses: Their Implications for Radiotherapy Treatment Planning. RSNA 2005 - online presentation. 2005. available from: <http://rsna2005.rsna.org/rsna2005/v2005/conference/dps.cfm>
7. Stambough JL, Genaidy AM, Huston RL et al: Biomechanical assessment of titanium and stainless steel posterior spinal constructs: effects of absolute/relative loading and frequency on fatigue life and determination of failure modes. *J Spinal Disord*, 1997; 10: 473-81
8. Cotterill PC, Kostuik JP, Wilson JA et al: Production of a reproducible spinal burst fracture for use in biomechanical testing. *J Orthop Res*, 1987; 5: 462-5
9. Korovessis PG, Magnissalis EA, Deligianni D: Biomechanical evaluation of conventional internal contemporary spinal fixation techniques used for stabilization of complete sacroiliac joint separation: a 3-dimensional unilaterally isolated experimental stiffness study. *Spine*, 2006; 31: E941-51
10. Reft C, Alecu R, Das IJ et al: Dosimetric considerations for patients with HIP prostheses undergoing pelvic irradiation. Report of the AAPM Radiation Therapy Committee Task Group 63. *Med Phys*, 2003; 30: 1162-82
11. Carolan M, Dao P, Fox C, Metcalfe P: Effect of hip prostheses on radiotherapy dose. *Australas Radiol*, 2000; 44: 290-5
12. Williams MV, Burnet NG, Sherwin E et al: A radiotherapy technique to improve dose homogeneity around bone prosthesis. *Sarcoma*, 2004; 8: 37-42
13. Biggs PJ, Russell MD: Effect of a femoral head prosthesis on megavoltage beam radiotherapy. *Int J Radiat Oncol Biol Phys*, 1988; 14: 581-86
14. Burlinson WD, Stutzman CD, Stitt JA et al: *In vivo* isocenter dose in two hip prosthesis patients. *Int J Radiat Oncol Biol Phys*, 1991; 20: 1347-52
15. Ding GX, Yu CW: A study on beams passing through hip prosthesis for pelvic radiation treatment. *Int J Radiat Oncol Biol Phys*, 2001; 51: 1167-75
16. Erlanson M, Franzen L, Henriksson R et al: Planning of radiotherapy for patients with hip prosthesis. *Int J Radiat Oncol Biol Phys*, 1991; 20: 1093-8
17. Roberts R: How accurate is a CT-based dose calculation on a pencil beam TPS for a patient with a metallic prosthesis? *Phys Med Biol*, 2001; 46: N227-34
18. Wieslander E, Knoos T: Dose perturbation in the presence of metallic implants: treatment planning system versus Monte Carlo simulations. *Phys Med Biol*, 2003; 48: 3295-305

19. Keall PJ, Siebers JV, Jeraj R, Mohan R: Radiotherapy dose calculations in the presence of hip prostheses. *Med Dosim*, 2003; 28: 107–12
20. Laub WU, Nusslin F: Monte Carlo dose calculations in the treatment of a pelvis with implant and comparison with pencil-beam calculations. *Med Dosim*, 2003; 28: 229–33
21. Lin SY, Chu TC, Lin JP, Liu MT: The effect of a metal hip prosthesis on the radiation dose in therapeutic photon beam irradiations. *Appl Radiat Isot*, 2002; 57: 17–23
22. Briesmeister JF: MCNP-A general Monte Carlo N-particle transport code, Version 4C. Report LA-13709-M. Los Alamos National Laboratory, NM, 2000
23. Mesbahi A, Thwaites D, Reilly A: Experimental and Monte Carlo evaluation of Eclipse treatment planning system for lung dose calculations. *Rep Pract Oncol Radiother*, 2006; 11 (3): 123–33
24. Mesbahi A, Fix M, Allahverdi M et al: Monte Carlo calculation of Varian 2300C/D Linac photon beam characteristics: a comparison between MCNP4C, GEANT3 and measurements. *Appl Radiat Isot*, 2005; 62: 469–77
25. Mesbahi A, Reilly AJ, Thwaites DI: Development and commissioning of a Monte Carlo photon beam model for Varian Clinac 2100EX linear accelerator. *Appl Radiat Isot*, 2006; 64: 656–62
26. Farajollahi A, Mesbahi A: Monte Carlo dose calculations for a 6-MV photon beam in a thorax phantom. *Radiat Med*, 2006; 24: 269–76